Spline-Based Distributed System Identification with Application to Large Space Antennas

H.T. Banks*
Brown University, Providence, Rhode Island
P.K. Lamm†
Southern Methodist University, Dallas, Texas
and
E.S. Armstrong‡
NASA Langley Research Center, Hampton, Virginia

A parameter and state estimation technique for distributed models is demonstrated through the solution of a problem generic to large space antenna system identification. Assuming the position of the reflective surface of the maypole (hoop/column) antenna to be approximated by the static two-dimensional, stretched-membrane partial differential equation with variable-stiffness coefficient functions, a spline-based approximation procedure is described that estimates the shape and stiffness functions from data set observations. For given stiffness funcions, the Galerkin projection with linear spline-based functions is applied to project the distributed problem onto a finite-dimensional subspace wherein algebraic equations exist for determining a static shape (state) prediction. The stiffness functions are then parameterized by cubic splines and the parameters estimated by an output error technique. Numerical results are presented for data descriptive of a 100-m-diameter maypole antenna.

Introduction

PROPOSED large space structures have many characteristics that make them difficult to analyze and control.[1] They are highly flexible—with components mathematically modeled by partial differential equations or vary large systems of ordinary differential equations. They have many resonant frequencies, typically low and closely spaced. The natural damping may be low and/or improperly modeled.[2] Coupled with stringent operational requirements of orientation, shape control, and vibration suppression, and the inability to perform adequate ground testing, these characteristics present an unconventional identification and control design problem to the systems theorist.

To date, the most popular control design approach appears to be the direct application of linear multivariable methodology to reduced-order lumped models obtained from finite element software; the goal of this approach is to control the structure so as to meet the operational requirements without overly exciting higher-order flexible modes. The effects of spillover, modeling error, and insufficient structural damping are well known[1,3] and may force the designer into low-authority control laws with compromised operational performance.

An alternative approach is to design the control system using distributed parameter techniques. Many methods exist in distributed parameter control theory that are analogous to those of multivariable theory.[1,4-9] Control laws derived from the distributed parameter theory are usually infinite-dimensional and often require significant simplification in order to be realized with current sensor and actuator technology.

The question of which control approach is best remains open and is essentially problem dependent.[10] However, when a distributed formulation is feasible for a given structure, it appears to have several advantages, particularly from a system identification viewpoint. A distributed model satisfies the fundamental need of the control theorist for a design and evaluation model that can be quickly and easily modified to carry out parametric studies and perform sensitivity and robustness analysis.[11,12] There are also many open questions in the understanding and modeling of damping[2,3] that may be better treated within a distributed parameter formulation. Finally, a distributed model appears to have the potential of facilitating the parameter estimation problem for large-scale systems, since the quantities to be estimated will usually appear concisely within the coefficient functions of the partial differential equations.

Within the collection of techniques available for system identification in distributed systems (for example, see Ref. 13), spline-based approximation methods appear well suited for application to large space structures. Banks et al.[14-19] have developed spline-based methods for approximating the solutions to identification and control problems involving delay and distributed models that are numerically attractive and on a sound theoretical basis. These methods have been tested in a variety of significant applicatioons,[20,21] although in areas not directly related to space. This paper describes our first attempt at applying these techniques to a class of problems containing large space structures. The spline-based methods are employed to produce a parameter and state estimation algorithm for a distributed model approximating the maypole (hoop/column) large space antenna reflector surface.[22,23]

The next section describes the spline-based system identification approach. The hoop/column antenna is then described along with the identification problem considered. Subsequent sections include mathmatical details of the antenna application and numerical results.

Received Sept. 10, 1985; revision received Jan. 20, 1986.

*Professor of Applied Mathematics, Lefshetz Center for Dynamical Systems.
†Assistant Professor, Department of Mathematics.
‡Senior Research Scientist, Spacecraft Control Branch, Guidance and Control Division.

System Identification Procedure

The first two authors and their colleagues have investigated techniques for approximating the solutions to systems identification and control problems involving partial differential equation models in one spatial variable. The applicaion herein requires an extension of the theory and numerical algorithms to elliptic-distributed systems in several spatial variables. The approach, when specialized to the identification problem, may be summarized as follows: 1) select a distributed parameter formulation containing unknown parameters for a specific application; 2) mathematically "project" the formulation down onto a finite-dimensional subspace through some approximation procedure such as finite differences, finite elements, etc.; 3) solve the identification problem within the finite-dimensional subspace obtaining estimates dependent upon the order of the approximation embodied in the subspace; 4) successively increase the order of the approximation and, in each case, solve the identification problem so as to construct a sequence of parameter and state estimates ordered with increasing refinement of the approximation scheme; and 5) seek a mathematical theory that provides conditions under which the approximate solutions approach the distributed solution as the sunspace dimension increases with a convergent underlying sequence of parameter estimates.

In the application to follow, the Galerkin procedure is used to project a distributed formulation onto a finite-dimensional state subspace spanned by tensor products of linear spline functions. The approximate distributed equation solution (state estimate) obtained within the subspace is thus expressible in terms of linear spline functions. An unknown distributed-model coefficient function is parameterized in terms of (fixed-order) cubic splines that convert its determination into a finite-dimensional parameter estimation problem. The Galerkin procedure yields equations that define the state estimate in terms of the unknown cubic spline parameters. In turn, these parameters are chosen so that a least squares measure of the fit error between the observed and predicted data is minimized. Finally, an algorithm is constructed to determine the order of the linear spline approximation above which little or no further improvement is obtained in the unknown parameters as one increases the dimension of the finite-dimensional subspace.

Application to Maypole Antenna

One of the planned activities of the NASA's Space Transportation System is the placement in Earth orbit of a variety of large space antennas. Potential missions will require antennas and structures in a large range of sizes (0.03-20 km). Applications include communications (mobile, trunking, etc.), remote sensing (soil moisture, salinity, etc.), deep space network (orbital relays), astronomy (x-ray, observatory, optical array, radio telescope, very long baseline interferometry, etc.), energy, and space platforms. Specific missions have been pinpointed and future requirements identified for large space antennas for communications, Earth sensing, and radio astronomy.[23] Particular emphasis is placed on mesh-deployable antennas in the 50-120-m-diameter category. One such antenna is the maypole (hoop/column) antenna shown for the 100-m point design in Figs. 1 and 2.

The hoop/column antenna consists of a knitted gold-plated molybdenum wire reflective mesh stretched over a collapsible hoop that supplies the rigidity necessary to maintain a circular outer shape. The mesh grid can be varied to meet a given radio frequency reflectivity requirement. The annular membrane-like reflector surface surrounds a telescoping mast that provides anchoring locations for the mesh center section (Fig. 1). The mast also provides anchoring for the cables that connect the top end of the mast to the outer hoop and the bottom end of the mast to 48 equally spaced radial graphite cord truss systems woven through the mesh surface.[22] Tensions on the upper (quartz) cables and outer lower (graphite epoxy) cables are counterbalanced to provide stiffness to the hoop structure. Through the truss systems, the inner lower cables produce surface loading to control the shape of four circular reflective dishes (Fig. 2) on the mesh surface. Flat, conical, parabolic, or spherical dish surfaces can be produced using this cable technique.

After deployment or after a long period of operation, the reflector surface may require adjustment. Optical sensors are located on the upper mast to measure the angles of retroreflective targets placed on the truss radial cord edges of the antenna surface. This information can then be processed using a ground-based computer to determine a data set of values of mesh surface location at selected target points. If necessary, a new set of shaping (control) cord tensions can be fed back to the antenna for adjustment.

What is desired is an identification procedure that allows the estimation of the antenna mesh shape at arbitary surface points and the loading from the data set observations. It can also be anticipated that environmental stresses and the effect of aging will alter the mesh material properties. The identification procedure must also allow this issue to be addressed.

The mesh cord construction of the reflector surface makes each gore a discontinuously nonhomogeneous, reinforced structure.[22] Also, it seems likely that the membrane tension is anisotropic within each mesh element and that the loading imposed by the cord trusses consists of discrete forces. Thus, derivation of a complete distributed model for the

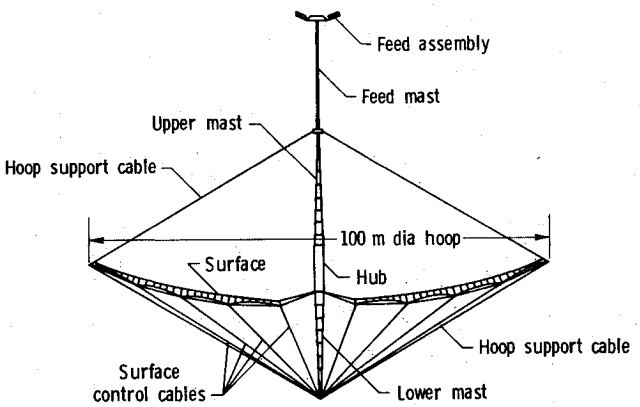

Fig. 1 Side view of maypole (hoop/column) antenna.

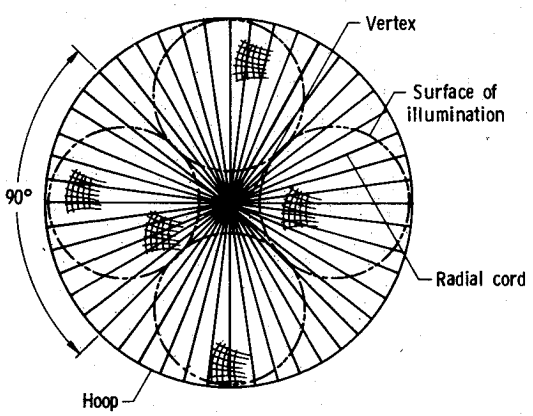

Fig. 2 Maypole (hoop/column) antenna reflector surface.

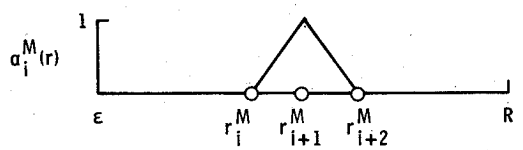

Fig. 3 Graphical representation of $\alpha_i^M(r)$, $(i=1,\ldots,M-1)$.

hoop/column reflector surface is a formidable task (for preliminary findings, see Ref. 24). The present study uses an idealized prototype model in which the reflector surface is treated as an isotropic, smoothly nonhomogeneous membrane under distributed loading. It is felt that this model permits the development and evaluation of the identification theory and algorithms that can later be extended to a more realistic case.

For the prototype model, the antenna is assumed to be fully deployed and in static equilibrium. A cylindrical coordinate system is employed with the z axis along the mast and positive direction toward the feed (see Fig. 2). The loading is assumed to be distributed (although discrete forces are easily handled by the method presented) and normal to the equilibrium plane containing the hoop rim. The mesh surface is described by the static two-dimensional, stretched-membane equation[25] with variable stiffness (elastic) coefficients and appropriate boundary conditions for the hoop/column geometry. Mathematically, in polar coordinates, this means

$$-\frac{1}{r}\frac{\partial}{\partial r}\left[rE(r,\theta)\frac{\partial u}{\partial r}\right]-\frac{1}{r^2}\frac{\partial}{\partial \theta}\left[E(r,\theta)\frac{\partial u}{\partial \theta}\right]=f(r,\theta) \quad (1)$$

where $u(r,\theta)$ is the vertical displacement of the mesh from the hoop plane, $f(r,\theta)$ the distributed loading force per unit area, and $E(r,\theta)>0$ the distributed stiffness coefficient of the mesh surface (force/unit length). Equation (1) is to be solved over the annular region $\Omega=[\epsilon,R]\times[0,2\pi]$. Appropriate boundary conditions are

$$u(\epsilon,\theta)=u_0, \quad u(R,\theta)=0, \quad u(r,0)=u(r,2\pi) \quad (2)$$

where R is the radius from the mast center to the circular outer hoop, ϵ the radius from the mast to the beginning of the mesh surface (see Fig. 2), and u_0 the coordinate at $r=\epsilon$ of the mesh surface below the outer hoop plane.

It is further assumed that the loading along with a data set of vertical displacements, $u_m(r_i,\theta_j)$, at selected points (r_i,θ_j), $i=1,\ldots,L_r$, $j=1,\ldots,L_\theta$, on the meash surface is known. Given this information, the considered identification problem is to estimate the material properties of the mesh as represented by $E(r,\theta)$ and to produce state estimates of the surface represented by $u(r,\theta)$ at arbitrary (r,θ) points within Ω.

Finite-Dimensional Approximations

Prior to applying the Galerkin procedure[26] to perform the finite-dimensional approximation for the prototype problem, the boundary conditions [Eq. (2)] are converted to homogeneous form by introducing the new dependent variable

$$y(r,\theta)=u(r,\theta)-\left(\frac{r-R}{\epsilon-R}\right)u_0 \quad (3)$$

Equation (1) becomes

$$-\frac{1}{r}\frac{\partial}{\partial r}\left[rE(r,\theta)\frac{\partial y}{\partial r}\right]-\frac{1}{r^2}\frac{\partial}{\partial \theta}\left[E(r,\theta)\frac{\partial y}{\partial \theta}\right]$$
$$=f(r,\theta)+\frac{1}{r}\frac{\partial}{\partial r}\left[\frac{rE(r,\theta)u_0}{\epsilon-R}\right] \quad (4)$$

with boundary conditions

$$y(\epsilon,\theta)=0, \quad y(R,\theta)=0, \quad y(r,0)=y(r,2\pi) \quad (5)$$

Following the standard formulation[26] for the weak or variational form of Eq. (4), the energy function $\mathcal{E}$ associated with Eq. (4) is

$$\mathcal{E}(z)=\int_0^{2\pi}\int_\epsilon^R [\tfrac{1}{2}E(r,\theta)\nabla z\cdot\nabla z-\tilde{f}(r,\theta)z]\,r\,dr\,d\theta \quad (6)$$

where ∇ is the gradient in polar coordinates that, in the form used here, is equivalent to

$$\left(\frac{\partial}{\partial r},\frac{1}{r}\frac{\partial}{\partial \theta}\right)^T \quad (7)$$

The function $\tilde{f}$ is given by

$$\tilde{f}(r,\theta)=f(r,\theta)+\frac{1}{r}\frac{\partial}{\partial r}\left(\frac{rE(r,\theta)u_0}{\epsilon-R}\right) \quad (8)$$

The vertical displacement $z(r,\theta)$ of the mesh surface from the hoop equilibrium plane is a function satisfying the boundary conditions [Eqs. (5)] and possessing first derivatives on Ω in the distributional sense. This is denoted by $z\epsilon H_{0,\,\mathrm{per}}(\Omega)$. The first variation $\delta\mathcal{E}$ of $\mathcal{E}$ about the funtion $y(r,\theta)$ is given by

$$\delta\mathcal{E}(y;v)=\int_0^{2\pi}\int_\epsilon^R [E(r,\theta)\nabla y\cdot\nabla v-\tilde{f}(r,\theta)v]\,r\,dr\,d\theta$$
$$=\int_0^{2\pi}\int_\epsilon^R \{E(r,\theta)\nabla y\cdot\nabla v-[f(r,\theta)v+E(r,\theta)\tilde{k}\cdot\nabla v]\}\,r\,dr\,d\theta \quad (9)$$

where

$$\tilde{k}=\begin{bmatrix}\hat{k}\\ 0\end{bmatrix}=\begin{bmatrix}\dfrac{u_0}{R-\epsilon}\\ 0\end{bmatrix} \quad (10)$$

and v is an arbitrary function in $Z=H^1_{0,\,\mathrm{per}}(\Omega)$.

Given a finite-dimensional subspace $\hat{Z}$ of Z, the Galerkin procedure defines the approximation $\hat{y}$ as the solution in $\hat{Z}$ of

$$\int_0^{2\pi}\int_\epsilon^R [E(r,\theta)\nabla\hat{y}\cdot\nabla\hat{v}]\,r\,dr\,d\theta$$
$$=\int_0^{2\pi}\int_\epsilon^R [f(r,\theta)\hat{v}+E(r,\theta)\tilde{k}\cdot\nabla\hat{v}]\,r\,dr\,d\theta \quad (11)$$

for all $\hat{v}\epsilon\hat{Z}$.

For computational efficiency, the basis functions used for the representations of $\hat{y}$ in Eq. (11) are taken as tensor products of linear "hat" or "roof" functions.[26,27] Thus, $\hat{v}$ and $\hat{y}$ are in the space spanned by $v_{ij}^{M,N}$, where

$$v_{ij}^{M,N}(r,\theta)=\alpha_i^M(r)\beta_j^N(\theta), \quad (i=1,\ldots,M-1; \quad j=1,\ldots,N) \quad (12)$$

where α_i^M and β_j^N have the form: on the interval $[\epsilon,\Delta]$ (subdivided by defining partition points $r_j^M=\epsilon+(R-\epsilon)\times(j-1)/M$, $j=1,\ldots,M+1$), α_i^M is the ith linear spline-basis element, $i=1,2,\ldots,M-1$, shown in Fig. 3. Subdividing $[0,2\pi]$ into intervals of uniform length $2\pi/N$ defines β_j^N for $j=1,\ldots,N-1$ and $\beta_N^N(\theta)$; see Figs. 4 and 5, respectively.

For $y(r,\theta)$ within the subspace spanned by $v_{ij}^{M,N}$

$$y^{M,N}(r,\theta)=\sum_{i=1}^{M-1}\sum_{j=1}^{N}\alpha_i^M(r)w_{ij}^{MN}\beta_j^N(\theta) \quad (13)$$

Note that the coordinate w_{ij}^{MN} is just the value of $y^{M,N}(r,\theta)$ *at*

$$r=\epsilon+\frac{i(R-\epsilon)}{M} \qquad (i=1,2,\ldots,M-1) \quad (14)$$

$$\theta=j2\pi/N \qquad (j=1,2,\ldots,N) \quad (15)$$

Replacing $\hat{y}(r,\theta)$ in Eq. (11) by $y^{M,N}(r,\theta)$ from Eq. (13) and successively setting $v(r,\theta)=v_{ij}^{M,N}(r,\theta)$ for $i=1,\ldots,M-1$ and $j=1,\ldots,N$ leads to a high-order linear sparse-matrix algebraic equation for the w_{ij}^{MN} coordinates.[28]

Sparse matrix methods are avoided in solving the w_{ij}^{MN} equation by imposing a separability condition,

$$E(r,\theta)=E_1(r)E_2(\theta) \tag{16}$$

Such an assumption as Eq. (16) facilitates the explanation of this method. Indeed, in the general case, one might wish to employ bivariate splines (or other appropriate multivariable approximation families) for the parameter approximation.

It is shown in Ref. 28 that Eq. (16) reduces the calculation of w_{ij}^{MN} to the solution of the matrix equation

$$\tilde{B}^M W^{MN}\tilde{A}^N+\tilde{D}^M W^{MN}\tilde{C}^N=\tilde{E}^{MN} \tag{17}$$

with

$$W^{MN}=(w_{ij}^{MN}) \tag{18}$$

$$\tilde{A}^N=\left(\int_0^{2\pi} E_2(\theta)\beta_i^N(\theta)\beta_j^N(\theta)\mathrm{d}\theta\right) \tag{19}$$

$$\tilde{B}^M=\left(\int_\epsilon^R E_1(r)\left[\frac{\mathrm{d}}{\mathrm{d}r}\alpha_i^M(r)\right]\left[\frac{\mathrm{d}}{\mathrm{d}r}\alpha_j^M(r)\right]r\mathrm{d}r\right) \tag{20}$$

$$\tilde{C}^N=\left(\int_0^{2\pi} E_2(\theta)\left[\frac{\mathrm{d}}{\mathrm{d}\theta}\beta_i^N(\theta)\right]\left[\frac{\mathrm{d}}{\mathrm{d}\theta}\beta_j^N(\theta)\right]\mathrm{d}\theta\right) \tag{21}$$

$$\tilde{D}^M=\left(\int_\epsilon^R E_1(r)\frac{\alpha_i^M(r)\alpha_j^M(r)}{r}\mathrm{d}r\right) \tag{22}$$

and

$$\tilde{E}^{MN}=\left(\int_0^{2\pi}\int_\epsilon^R f(r,\theta)\alpha_i^M(r)\beta_j^N(\theta)r\mathrm{d}r\mathrm{d}\theta + \int_0^{2\pi}\int_\epsilon^R E(r,\theta)\hat{k}\beta_j^N(\theta)\left[\frac{\mathrm{d}}{\mathrm{d}r}\alpha_i^M(r)\right]r\mathrm{d}r\mathrm{d}\theta\right) \tag{23}$$

where in Eqs. (18-23), $\tilde{A}^N$ and $\tilde{C}^N$ are $N\times N$, $\tilde{B}^M$ and $\tilde{D}^M$ are $(M-1)\times(M-1)$, and W^{MN} and $\tilde{E}^{MN}$ are $(M-1)\times N$. The matrices of Eqs. (19-23) are symmetric with Eqs. (19) and (22) positive definite and Eqs. (20-22) tridiagonal.

For computational purposes, Eq. (17) is rewritten in the equivalent Sylvester equation form

$$[(\tilde{D}^M)^{-1}\tilde{B}^M]W^{MN}+W^{MN}[\tilde{C}^N(\tilde{A}^N)^{-1}]=(\tilde{D}^M)^{-1}\tilde{E}^{MN}(\tilde{A}^N) \tag{24}$$

and solved by the Bartels-Stewart algorithm.[29]

In order to estimate, via a numerical scheme, the functional coefficients $E_1(r)$ and $E_2(\theta)$, these functions are parameterized so that the identification is performed over a finite-dimensional parameter set. To this end, let

$$E_1^{M_1}(r)=\sum_{k=1}^{M_1}\nu_k^{M_1}\lambda_k^{M_1}(r) \tag{25}$$

$$E_2^{N_1}(\theta)=\sum_{j=1}^{N_1}\delta_j^{N_1}\mu_j^{N_1}(\theta) \tag{26}$$

where $\nu_k^{M_1}$ and $\delta_j^{N_1}$ are scalar parameters and $\lambda_k^{M_1}$ and $\mu_j^{N_1}$ are cubic B-spline functions[27] whose orders are indepenent of M and N defined over $[\epsilon,R]$ and $[0,2\pi]$, respectively. The basic spline functions are modified so that μ_j satisfies the periodic boundary conditions. Note that this second level of approximation, introduced through parameterization of E_1 and E_2, must be included in any theoretical convergence study (see Refs. 19 and 28). In order to simplify the presentation here (and since M_1 and N_1 are usually fixed in practice), simply write $E_1=E_1^{M_1}$, $E_2=E_2^{N_1}$, $\nu_k=\nu_k^{M_1}$, etc., throughout. Using Eqs. (25) and (26),

$$\tilde{A}^N=\sum_{k=1}^{N_1}\delta_k\tilde{A}_k^N \tag{27}$$

$$\tilde{B}^M=\sum_{k=1}^{M_1}\nu_k\tilde{B}_k^M \tag{28}$$

$$\tilde{C}^N=\sum_{k=1}^{N_1}\delta_k\tilde{C}_k^N \tag{29}$$

$$\tilde{D}^M=\sum_{k=1}^{M_1}\nu_k\tilde{D}_k^M \tag{30}$$

where

$$\tilde{A}_k^N=\left(\int_0^{2\pi}\mu_k(\theta)\beta_i^N(\theta)\beta_j^N(\theta)\mathrm{d}\theta\right) \tag{31}$$

$$\tilde{B}_k^M=\left(\int_\epsilon^R\lambda_k(r)\left[\frac{\mathrm{d}}{\mathrm{d}r}\alpha_i^M(r)\right]\left[\frac{\mathrm{d}}{\mathrm{d}r}\alpha_j^M(r)\right]r\mathrm{d}r\right) \tag{32}$$

$$\tilde{C}_k^N=\left(\int_0^{2\pi}\mu_k(\theta)\left[\frac{\mathrm{d}}{\mathrm{d}\theta}\beta_i^N(\theta)\right]\left[\frac{1}{\mathrm{d}\theta}\beta_j^N(\theta)\right]\mathrm{d}\theta\right) \tag{33}$$

$$\tilde{D}_k^M=\left(\int_\epsilon^R\lambda_k(r)\frac{\alpha_i^M(r)\alpha_j^M(r)}{r}\mathrm{d}r\right) \tag{34}$$

Also

$$\tilde{E}^{MN}=\left(\int_0^{2\pi}\int_\epsilon^R f(r,\theta)\alpha_i^M(r)\beta_j^N(\theta)r\mathrm{d}r\mathrm{d}\theta + \hat{k}\left[\sum_{k=1}^{N_1}\delta_k\int_0^{2\pi}\mu_k(\theta)\beta_j^N(\theta)\mathrm{d}\theta\right] \times\left[\sum_{k=1}^{M_1}\nu_k\int_\epsilon^R\lambda_k(r)r\frac{\mathrm{d}}{\mathrm{d}r}\alpha_i^M(r)\mathrm{d}r\right]\right) \tag{35}$$

The computer implementation of the indentification procedure is outlined in the next section.

Computational Procedure

Appealing to the ideas found in previous sections, an algorithm can be constructed for estimating the coefficients ν_k $(k=1,\ldots,M_1)$ and δ_j $(j=1,\ldots,N_1)$ in the parametric representations for $E(r,\theta)$ that provide the "best fit" between the estimations for state u and the observed data u_m obtained from various sample points on the surface. The data for y may be equivalently considered by making the transformation

$$y_m(r_i,\theta_j)=u_m(r_i,\theta_j)-\left(\frac{r_i-R}{\epsilon-r}\right)u_0 \tag{36}$$

for $i=1,\ldots,L_r$, and $j=1,\ldots,L_\theta$.

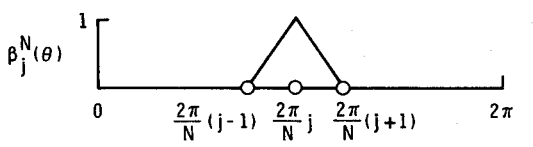

Fig. 4 Graphical representation of $\beta_j^N(\theta)$, $(j=1,\ldots,N-1)$.

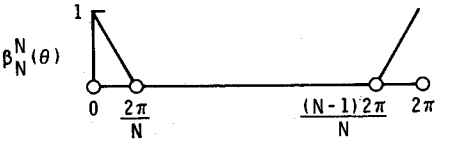

Fig. 5 Graphical representaion of $\beta_N^N(\theta)$.

The parameter and state estimation algorithm is organizied into the following steps:

1) Select an order of approximation for the cubic spline elements λ_k $(k=1,\ldots,M_1)$ and μ_j $(j=1,\ldots,N_1)$ used to represent E_1 and E_2. Set $n=1$. Note that the selection of M, N, M_1, and N_1 is highly problem dependent and that this choice is often guided by experience with model numerical problems. For an example of such choices, the reader is referred to the numerical results of the next section.

2) Select M and N, the orders of the linear spline-based elements used to represent $u^{M,N}$ (and $y^{M,N}$).

3) Assume a nominal set of values ν^0 and δ^0 for

$$\nu=(\nu_1,\nu_2,\ldots,\nu_{M_1}) \tag{37}$$

and

$$\delta=(\delta_1,\delta_2,\ldots,\delta_{N_1}) \tag{38}$$

The δ^0 and ν^0 values are typically the coefficients in a cubic spline interpolation for an initial guess of the shape of E_1 and E_2.

4) Calculate the coefficient matrices in Eq. (24) and solve for $W^{MN}(\nu,\delta)$.

5) From Eq. (13), calculate $y^{M,N}(r_i,\theta_j;\nu,\delta)$ and evaluate

$$J^{MN}(\nu,\delta)=\sum_{i=1}^{L_r}\sum_{j=1}^{L_\theta}[y^{M,N}(r_i,\theta_j;\nu,\delta)-y_m(r_i,\theta_j)]^2 \tag{39}$$

6) Proceed to step 8 if $J^{MN}(\nu,\delta)$ is sufficently small. Otherwise, through an optimization procedure (e.g., modified Newton algorithm, gradient method, etc.), determine a new (ν,δ) pair that decreases the value of J^{MN}. If no such pair can be found, go to step 8.

7) Set $(\nu,\delta)=(\hat{\nu},\hat{\delta})$ and return to step 4.

8) Preserve the current values of J^{MN} and the corresponding (ν,δ) pair as the nth entry in a sequence ordered with increasing M and N.

9) Proceed to step 10 if sufficient data have been obtained to analyze the sequences. Otherwise, replace n with $n+1$ and return to step 2 with increased M and N using the current values of (ν,δ) as nominal values for the next optimization process.

10) From analysis of the numerical sequences, select the M,N entry that indicates the best numerical results. The corresponding (ν,δ) pair yields $E(r,\theta)$, determining the material properties of the antenna mesh. The matrix $W^{MN}(\nu,\delta)$, when used in conjunction with Eq. (13), determines a state approximation $y^{M,N}$ of the shape of the antenna surface.

A convergence theory for the identification algorithm may be found in Ref. 28. Numerical results are described in the next section.

Numerical Results

Experimental data for the hoop/column antenna are not available at this time. Therefore, synthetic data were constructed to demonstrate the efficacy of the preceding algorithm. These data were constructed as follows.

As shown in Fig. 2, the parent reflector has four separate areas of illumination on its surface. Each area is assumed to have the same parabolic shape. For $0\le\theta\le\pi/2$ and $\epsilon\le r\le R$,

$$u^0(r,\theta)=\begin{cases}\dfrac{u_0(R-r)}{R-\epsilon}\left[k\left(\dfrac{r-\epsilon}{R}\right)q_2(\theta)+1\right], & 0\le\theta\le\dfrac{\pi}{36}\\[2ex]\dfrac{u_0(R-r)}{R-\epsilon}\left[k\left(\dfrac{r-\epsilon}{R}\right)q_1(\theta)+1\right], & \dfrac{\pi}{36}\le\theta\le\dfrac{17\pi}{36}\\[2ex]\dfrac{u_0(R-r)}{R-\epsilon}\left[k\left(\dfrac{r-\epsilon}{R}\right)q_3(\theta)+1\right], & \dfrac{17\pi}{36}\le\theta\le\dfrac{\pi}{2}\end{cases} \tag{40}$$

where

$$q_1(\theta)=\sin\theta+\cos\theta \tag{41}$$

The functions $q_2(\theta)$ and $q_3(\theta)$ are cubic polynomial fits used to ensure smoothness in regions of θ near $\theta=\pi/2$, π, $3\pi/2$, and 2π. Formulas for $q_2(\theta)$ and $q_3(\theta)$ may be found in Ref. 28. The parameter $k>0$, a stretch factor used to perturb the surface below the conic $(k=0)$ shape, is taken as 0.25.

For the complete surface, define, for $\epsilon\le r\le R$,

$$u(r,\theta)=\begin{cases}u^0(r,\theta), & 0\le\theta\le\pi/2\\ u^0\left(r,\theta-\dfrac{\pi}{2}\right), & \pi/2\le\theta\le\pi\\ u^0(r,\theta-\pi), & \pi\le\theta\le 3\pi/2\\ u^0\left(r,\theta-\dfrac{3\pi}{2}\right), & 3\pi/2\le\theta\le 2\pi\end{cases} \tag{42}$$

It is expected that the mesh will be stiffest near the outer hoop $(r=R)$ and around the inner radius $(r=\epsilon)$. For this reason, a known value of $E_1(r)$ is chosen

$$\bar{E}_1(r)=2\hat{\tau}-\hat{\tau}\sin\left[\pi\frac{(r-\epsilon)}{(R-\epsilon)}\right], \qquad \epsilon\le r\le R \tag{43}$$

where $\hat{\tau}$ is a constant dependent on the mesh material. The stiffness in the angular direction is taken to be uniform with

$$\bar{E}_2(\theta)\equiv\hat{\tau} \tag{44}$$

From data provided in Ref. 22 for the 100-m point design, a value for $\hat{\tau}$ (given in units $\sqrt{N/m}$) is taken as

$$\hat{\tau}=3.391 \tag{45}$$

Similarly, other parameters are calculated to be $\bar{u}_0=-7.5$ m, $\epsilon=8.235$ m, and $R=50$ m.

A 10×24 grid of data points $u_m(r_i,\theta_j)$ is calculated by evaluating $\bar{u}(r,\theta)$ at points (r_i,θ_j) with

$$r_i=\epsilon+i\frac{(R-\epsilon)}{11}, \qquad i=1,2,\ldots,L_r=10 \tag{46}$$

$$\theta_j=[7.5^\circ+(j-1)15^\circ]\frac{\pi}{180}, \quad j=1,2,\ldots,L_\theta=24 \tag{47}$$

Values of θ_j correspond to data taken along every other radial cord truss system with reflectors located on the gore edges. Distributed loads are obtained by substituting Eqs. (42-44) into Eq. (1) and evaluating $f(r,\theta)$.

In the examples of the identification process to be presented, an equal number of linear spline-based functions are used in both r and θ directions. That is, $M=N+1$ for an increasing sequence of N values. The cubic spline approximations [Eqs. (25) and (26)] are used with fixed $M_1=N_1=4$ to represent E_1(r) and $E_2(\theta)$. The International Mathematical and Statistical Library (IMSL) version (ZXSSQ) of the Levenberg-Marquardt algorithm[30] with numerical gradients is employed to minimize J^{MN} given by Eq. (39). For the first choice of N, nominal (ν,δ) parameter values used to initialize the Levenberg-Marquardt algorithm are obtained by finding those (ν,δ) coordinates that cause Eqs. (25) and (26) to best approximate the assumed functions $E_1^0(r)$ and $E_2^0(\theta)$ chosen as guessed froms of $\bar{E}_1(r)$ and $\bar{E}_2(\theta)$, respectively. For larger N, the latest previously obtained set of converged coordinates is used as the nominal parameters. Numerical calculations were performed on a CDC Cyber 170 series digital computer using default values of the IMSL convergence parameters.

Two measures of identification scheme performance are employed. The quantity

$$\hat{J}^{MN} = \left(\frac{J^{MN}}{L_r L_\theta}\right)^{1/2} \tag{48}$$

is used as a measure of state estimation accuracy. Additionally

$$R^{MN} = \frac{|E^{MN} - \bar{E}|}{|\bar{E}|} \times 100\% \tag{49}$$

measures the relative error between the true

$$\bar{E}(r,\theta) = \bar{E}_1(r)\bar{E}_2(\theta) \tag{50}$$

and the estimated $E(r,\theta)$ denoted by

$$E^{MN}(r,\theta) = E_1^{MN}(r)E_2^{MN}(\theta) \tag{51}$$

which is calculated from Eqs. (25) and (26) using (with $M_1 = N_1 = 4$ fixed) the (M,N)th level of state approximation obtained at step 8 of the computational procedure. In Eq. (49), $|\cdot|$ denotes the L_2 norm on $[\epsilon,R] \times [0,2\pi]$. R^{MN} provides a measure of parameter estimation accuracy.

Convergence in the sense that

$$R^{MN} \to 0 \text{ and } \hat{J}^{MN} \to 0 \text{ as } (M,N) \to \infty \tag{52}$$

depends on the ability of the cubic spline approximates $E_1(r)$ and $E_2(\theta)$ in Eqs. (25) and (26) to accurately represent $\bar{E}_1(r)$ and $\bar{E}_2(\theta)$. In this case, $\bar{E}_2(\theta)$ can be represented by the δ coefficients: $\bar{\delta}_i = 0.5652$, $(i = 1,\ldots,4)$. However, the best approximation $E_1(r)$ for $\bar{E}_1(r)$ using Eq. (25) and $M_1 = 4$ uses the ν coefficients $\bar{\nu} = (5.026, 0.3833, 0.3833, 5.026)$ and leads to

$$\frac{|E_1(r) - \bar{E}_1(r)|}{|\bar{E}_1(r)|} = 1.23\% \tag{53}$$

relative error. Consequently, entries in the $(R^{MN}, \hat{J}^{MN})$ sequence can be expected to cease decreasing past some (M,N) value. Other examples in which Eqs. (25) and (26) exactly fit simpler $\bar{E}_1(r)$ and $\bar{E}_2(\theta)$ functions and $\hat{J}^{MN}$ and R^{MN} monotonically decrease with increasing (M,N) can be found in Ref. 28. Also, using the best cubic spline fits to $\bar{E}_1(r)$ and $\bar{E}_2(\theta)$ to define $E(r,\theta)$, along with the exact $f(r,\theta)$ data, it is observed that

$$\hat{J}^{MN} \approx 0.087 \tag{54}$$

uniformly in (M,N). The following numerical results show that the parameter estimates from the identification procedure tend to improve (reduce) this $\hat{J}^{MN}$ value at the expense of R^{MN}.

Example 1

Estimate $E_2(\theta)$ holding $E_1(r)$ fixed, i.e., determine δ while holding $\nu = \bar{\nu}$ fixed at

$$\nu = (5.026,\ 0.3833,\ 0.3833,\ 5.026) \tag{55}$$

Nominal parameters for the $N = 4$ starting value are obtained by fitting Eq. (26) to

$$E_2^0(\theta) = 1 + \tfrac{1}{2}\cos\theta \tag{56}$$

yielding

$$\delta^0 = (0.1667,\ 0.2933,\ 0.1667,\ 0.0398) \tag{57}$$

Four δ parameters are estimated with results summarized below in Table 1.

Table 1 Results from estimating $E_2(\theta)$ with $E_1(r)$ fixed

N	$\hat{J}^{MN}$, m	R^{MN}, %
4	0.0390	5.13
6	0.0384	5.57
8	0.0322	5.69
10	0.0347	6.01
12	0.0330	5.83

Table 2 Results from estimating $E_1(r)$ with $E_2(\theta)$ fixed

N	$\hat{J}^{MN}$, m	R^{MN}, %
4	0.0355	32.25
6	0.0343	24.5
8	0.0270	4.39
10	0.0293	13.17
12	0.0275	8.08
14	0.0273	7.44
16	0.0271	7.59
18	0.0267	7.68
20	0.0264	8.03
22	0.0260	7.91
24	0.0267	8.11
26	0.0250	7.49
28	0.0203	7.58
30	0.0259	7.71

Essentially no improvement in state estimate was obtained past $N = 8$ with

$$\delta_i = 0.5969, \qquad i = 1,\ldots,4 \tag{58}$$

The estimated $E^{MN}(\theta)$ tended to 3.591 instead of the true value $\bar{E}_2(\theta) \times = 3.391$. The ≈ 0.20 bias is attributed to the inability of Eq. (25) to exactly fit $\bar{E}_1(r)$.

The divergence observed when moving from $N = 8$ to $N = 10$ is probably due to the fact that at $N = M - 1 = 10$, the nodal points [Eq. (14)] coincide with the data set [Eq. (46)]. Because of the "quadrant symmetry" of $u(r,\theta)$, the 8×8 coordinate matrix W^{MN} for $N = 8$ to be used to construct the approximate state estimator via Eq. (13) is given by four equal 8×2 column blocks given by

$$\begin{bmatrix} -0.2309 & -0.2242 \\ -0.3844 & -0.3687 \\ -0.4755 & -0.4504 \\ -0.5189 & -0.4840 \\ -0.5176 & -0.4726 \\ -0.4632 & -0.4112 \\ -0.3505 & -0.3004 \\ -0.1887 & -0.1546 \end{bmatrix} \tag{59}$$

Example 2

Estimate $E_1(r)$ holding $E_2(\theta)$ fixed at $\bar{E}_2(\theta)$ with $\delta = \bar{\delta}$ and

$$\delta_i = 0.5652, \qquad i = 1,\ldots,4 \tag{60}$$

Nominal parameters ν^0 for the $N = 4$ starting value are obtained by fitting Eq. (25) to

$$E_1^0(r) \equiv 1 \tag{61}$$

yielding

$$\nu_i^0 = 0.1667, \qquad i = 1,\ldots,4 \tag{62}$$

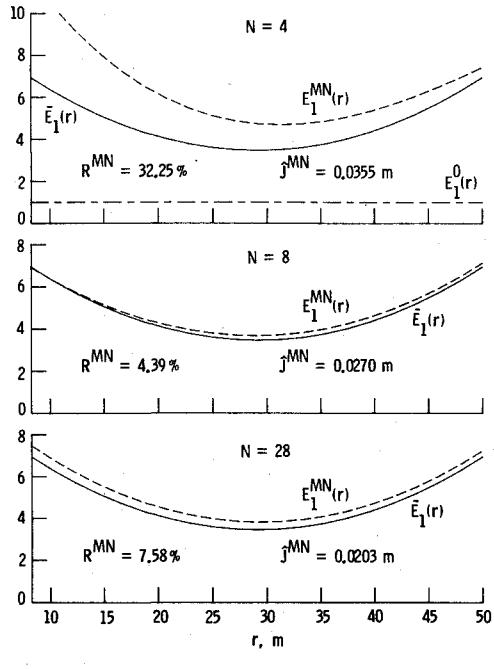

Fig. 6 Estimate $E_1(r)$ with $E_2(\theta)$ fixed.

Four ν parameters are estimated with results summarized below in Table 2. Figure 6 shows the character of $E_1^{MN}(r)$ for selected values of N. From a state estimation viewpoint, $N=28$ provides the best accuracy. Overall, considering state, parameter, and ease of comptuation, $N=8$ is judged best with

$$\nu = (4.771,\ 0.4282,\ 0.4269,\ 4.992) \tag{63}$$

Even though Eq. (63) differs from Eq. (55) [in order to reduce $\hat{J}$ below the value given in Eq. (54)], Fig. 6 shows that $E_1^{MN}(r)$ accurately describes $\bar{E}_1(r)$. For $N=8$, W^{MN} has the same construction as in example 1 with the first two columns given by

$$\begin{bmatrix} -0.2178 & -0.2107 \\ -0.3623 & -0.3462 \\ -0.4538 & -0.4284 \\ -0.5080 & -0.4728 \\ -0.5223 & -0.4781 \\ -0.4840 & -0.4317 \\ -0.3775 & -0.3268 \\ -0.2088 & -0.1742 \end{bmatrix} \tag{64}$$

Example 3

Estimate both $E_1(r)$ and $E_2(\theta)$. Nominal parameters are obtained as before with $N=4$ from

$$E_1^0(r) \equiv 5 \tag{65}$$

yielding

$$\nu_i^0 = 0.8333, \qquad i=1,\ldots,4 \tag{66}$$

and

$$E_2^0(\theta) = 1 - \tfrac{1}{2}\sin\theta \tag{67}$$

yielding

$$\delta^0 = (0.2300,\ 0.1667,\ 0.1033,\ 0.1667) \tag{68}$$

For each N, the first element of Eq. (38), δ_1, is held fixed at its initial value δ_1^0. Seven parameters are estimated again producing $N=8$ as best value, resulting in

$$\nu = (11.74,\ 1.050,\ 1.051,\ 12.26) \tag{69}$$

$$\delta_i = 0.2300, \qquad i=1,\ldots,4 \tag{70}$$

Convergence properties are similar to those of example 2, but with longer execution times due to the increased number of parameters involved. The $\delta_i\,(i=1,\ldots,4)$ converged quickly to Eq. (70) and therefore remained fixed while the algorithm concentrated on obtaining Eq. (69). After a few initial iterations, example 3 thus becomes a version of example 2 and, as should be expected from the seperable form of Eq. (16), the converged parameters of Eqs. (69) and (70) produce the same values of $E^{MN}(r,\theta)$ as was found in example 2.

In each example, we were able to successfully estimate the surface shape of the model antenna. Similar results have been obtained where random noise (approximately 5% noise level) has been added to the data. These and other findings may be found in Sec. VI of Ref. 28.

Conclusions

A general framework for system identification in distributed parameter systems has been presented. Approximations based on families of spline functions have been used to illustrate application of the ideas for a prototype large space antenna problem. The method successfully estimated the idealized antenna reflector surface shape and stiffness properties within the limits allowed by the spline basis functions. While the spline approximations perform well for the simple examples considered, continuing investigations within this framework using other approximation ideas (multigrid, spectral families) suggest that for more complicated, spatially distributed structures, generalizations of the overall approach will be more fruitful. Also currently under investigation is the use of algorithms for vector and parallel computers to meet the increased computational burdens that will be present in more complex structures.

Acknowledgments

Reserach reported here was supported in part by NASA Grant NAG-1-258 for the first and second authors, in part by National Science Foundation Grant MCS-8205355 and in part by U.S. Air Force Office of Scientific Research Grant 81-0198 for the first author and NSF Grant MCS-8200883 for the second author. Parts of the efforts reported were carried out while the first two authors were in residence at the Institute for Computer Applications in Science and Engineering, NASA Langley Research Center, Hampton, VA, which is operated under NASA Contracts NAS1-15810 and NAS1-16394.

References

[1]Balas, M.J., "Trends in Large Space Structure Control Theory: Fondest Hopes, Wildest Dreams," *IEEE Transactions on Automatic Control,* Vol. AC-27, June 1982, pp. 522-535.

[2]Hughes, P.C., "Passive Dissipation of Energy of Large Space Structures," *Journal of Guidance and Control,* Vol. 3, 1980, pp. 380-382.

[3]Gran, R. and Rossi, M., "A Survey of the Large Space Structures Control Problem," *Proceedings of IEEE Decision and Control Conference,* IEEE, New York, 1979.

[4]Lions, J.L., *Optimal Control of Systems Governed by Partial Differential Equations,* Springer-Verlag, New York, 1971.

[5]Russell, D., "Controllability and Stabilizability Theory for Linear PDE's: Recent Progress and Open Questions," *SIAM Review,* Vol. 20, 1978, pp. 638-739.

[6]Balakrishnan, A.V., *Applied Functional Analysis,* 2nd ed., Springer-Verlag, New York, 1981.

[7]Curtain, R.F. and Pritchard, A.J., *Infinite Dimensional Linear System Theory,* Springer-Verlag, New York, 1978.

[8]Ray, W.H. and Lainoiotis, D.G., (eds.) *Distributed Parameter Systems: Identification, Estimation, and Control,* Marcel Dekker, New York, 1978.

[9]Gibson, J.S., "An Analysis of Optimal Modal Regulation: Convergence and Stability," *SIAM Journal on Control and Optimization,* Vol. 19, 1981, pp. 686-707.

[10]Rodriguez, G., (ed.), *Proceedings of the Workshop on Applications of Distributed System Theory to the Control of Large Space Structures,* Jet Propulsion Laboratory, Calfornia Institute of Technology, Pasadena, CA, July 1, 1983.

[11]Johnson, T.L., "Progress in Modelling and Control of Flexible Spacecraft," *Journal of the Franklin Institute,* Vol. 315, 1983, pp. 495-520.

[12]Special Issue on Linear Multivariable Control Systems, *IEEE Transations on Automatic Control,* Vol. AC-26, Feb. 1981.

[13]Polis, M.P., "The Dsitributed System Parameter Identificaiton Problem: A Survey of Recent Results," *Proceedings of the IFAC Third Symposium on Control of Distributed Parameter Systems,* Pergamon Press, New York, 1982, pp. 45-58.

[14]Banks, H.T., "Algorithms for Estimation in Distributed Models with Applications to Large Space Structures," *Proceedings of Workshop on Applications of Distributed System Theory to the Control of Large Space Structures,* Jet Propulsion Laboratory, California Institute of Technology, Pasadena, CA, July 1982.

[15]Banks, H.T. and Crowley, J.M., "Parameter Estimation in Timoshenko Beam Models," *Journal of the Astronautical Sciences,* Vol. 31, 1983, pp. 381-397.

[16]Banks, H.T., Crowley, J.M., and Kunisch K., "Cubic Spline Approximation Techniques for Parameter Estimation in Distributed Systems," *IEEE Transactions on Automatic Control,* Vol. AC-28, July 1983, pp. 773-786.

[17]Banks, H.T. and Daniel, P.L., "Parameter Estimation of Nonlinear Nonautonomous Distributed Systems," *Proceedings 20th IEEE Conference on Decision and Control,* IEEE, New York, Dec. 1981, pp. 228-232.

[18]Banks, H.T. and Kunisch, K., "An Approximation Theory for Nonlinear Partial Differential Equations with Applications to Identification and Control," *SIAM Journal on Control and Optimization,* vol. 20, 1982, pp. 815-849.

[19]Banks, H.T. and Lamm, P.D., "Estimation of Variable Coefficients in Parabolic Distributed Systems," *IEEE Transactions on Automatic Control,* Vol. AC-30, April 1985, pp. 386-398.

[20]Banks, H.T., "Distributed Systems Optimal Control and Parameter Estimation: Computational Techniques Using Spline Approximations," *Proceedings of the IFAC Third Symposium on Control of Distributed Parameter Systems,* 1982, pp. SP21-SP27.

[21]Banks, H.T., "A Survey of Some Problems and Recent Results for Parameter Estimation and Control in Delay and Distributed Parameter Systems," *Volterra and Functional Differential Equations,* Marcel Dekker, New York, 1982, pp. 3-24.

[22]Sullivan, M.R., "LSST (Hoop/Column) Maypole Antenna Development Program, Parts I and II," NASA CR 3558, June 1982.

[23]Russell, R.A., Campbell, T.G., and Freeland, R.E., "A Technology Development Program for Large Space Antennas," Paper IAF-80A33 presented at the 31st International Astronautical Congress of the International Astronautical Federation, Tokyo, Sept. 1980.

[24]Banks, H.T. and Majda, G., "Modelling of Flexible Surfaces: A Preliminary Study," *Mathematical Modelling,* Vol. 5, 1984, pp. 103-115.

[25]Sagan, H., *Boundary and Eigenvalue Problems in Mathematical Physics,* John Wiley & Sons, New York, 1966.

[26]Stang, G. and Fix, G.J., *An Analysis of the Fintie Element Method,* Prentice-Hall, Englewood Cliffs, NJ, 1973.

[27]DeBoor, C., *A Practical Guide to Splines,* Applied Mathematical Sciences Series, Vol. 27, Springer-Verlag, New York, 1978.

[28]Banks, H.T., Daniel, P.L., and Armstrong, E.S., "A Spline-Based Parameter and State Estimation Technique for Static Models of Elastic Surfaces,' NASA Langley Research Center, Hampton, VA, ICASE Rept. 83-25, June 1983.

[29]Bartels, R.H. and Stewart, G.W., "Algorithm 432: Solution of the Matrix Equation $AX+XB=C$," *Communications of the ACM,* Vol. 15, Sept. 1972, pp. 820-826.

[30]Moré, J.J., "The Levenberg-Marquardt Algorithm," *Implementation and Theory in Numerical Analysis, Lecture Notes in Mathematics,* Vol. 630, Springer-Verlag, New York, 1977.